Fresnel Field to Far Field Transformation Based on Two-Dimensional Fourier Series Expansion

Yury V. Krivosheev, Alexander V. Shishlov, Aleksey K. Tobolev and Irina L. Vilenko

Company "Radiofizika", Moscow, Russia
E-mail: jscapex@online.ru

Abstract

A method of Fresnel field to far field transformation based on two-dimensional Fourier series expansion is presented. According to the method, far field can be reconstructed from several sections of the field in Fresnel region. Computer simulation and experimental verification results are given. Relationship to other results of antenna measurements theory is considered.

1. Introduction

Reconstruction of antenna characteristics from Fresnel region measurements is an important problem of the antenna engineering. Particularly, it is important when one has an anechoic chamber with test facility for far field measurements, but far field distance of an antenna under test (AUT) is larger than the length of an anechoic chamber.

For far field reconstruction from measurements in Fresnel region classical methods of far-field reconstruction from near-field measurements can be used. It is known that in this case measurements can be carried out only in a limited angular sector [1,2]. However, it requires $\lambda/2$ spacing between samples, so the amount of measurements can be large.

In the literature several methods of far field reconstruction specific to Fresnel region have been proposed. In these methods the spacing between samples is much larger than $\lambda/2$, which allows to reduce measurements time.

In [3,4] a solution of three-dimensional problem based on pseudosampling representation of the field was found. The presented method is convenient for both computation and practical realization. A disadvantage of the method is that the far field can be reconstructed only in angular directions close to the normal of the aperture.

In [5,6] a method based on one-dimensional Fourier series expansion of phase exponential was presented. The solution is also convenient to use (e.g. [7]), but is applicable only to linear antennas elongated in one direction, because in [5,6] only a two-dimensional problem was considered. However, the method is not limited only to the directions close to the normal of the aperture.

In [8] a generalization of [5,6] to three-dimensional case based on Bessel functions expansion was considered. The proposed representation is less convenient in practical sense, because it requires to measure field in an irregular angular grid.

In [9] a solution to three-dimensional problem based on [5,6] was proposed, which utilizes two-dimensional Fourier series expansion. As opposed to Bessel functions expansion, this method requires to carry out measurements in a regular angular grid, which makes it convenient to use in practice. Also, for the directions close to the normal of the aperture the expansion presented in [9] tends to the expansion in [4]. Thus, a method of two-dimensional Fourier series expansion can be considered as a generalization of method [4] for reconstruction of the far field in the directions which are not close to the normal of the aperture. Also in [9] several issues concerning practical implementation of the method were discussed.

Method [9] was further developed in papers [10–12], where measurements on non-spherical surface were considered [10], a Fresnel field to Fresnel field transformation was presented [11] and an alternative approach to expansion coefficients calculation was given for far field reconstruction from measurements at smaller distances [12].

In the current paper a method of Fresnel field to far field transformation based on two-dimensional Fourier series expansion is presented [9]. New results are given, such as vector form of the formulas for arbitrary point in far zone (in [9] only points with either small azimuth or small elevation were considered) and relationship of the method to other results of antenna measurements theory. Formulas for such characteristics as gain and EIRP and configuration of the measurement system are presented. Also the results of numerical simulation and experimental verification are given.

2. Mathematical model

Consider an antenna with dimensions at least several wavelengths. Let the antenna be in the left half-space near the z=0 plane (Fig.1). Then we need to choose a rectangle T_xxT_y in the z=0 plane, which must be at least as large as the antenna. Also let the antenna be positioned in such way that the center of the rectangle coincides with the origin.

To describe the field at z>0 mathematically we'll use Kirchhoff integral with the Green's function, chosen to eliminate either the term with the derivative of the field, or the term with the field. Also the field at z=0 outside the

T_xxT_y rectangle is neglected. Then the electric field in an arbitrary point in the right half-space for which $kr \gg 1$ can be written in terms of the field at z=0 plane as:

$$\mathbf{E}(u,v,r) = j \iint_{T_x \times T_y} \mathbf{E}(x,y,0) \times \frac{W(x,y)e^{-jkR(x,y)}}{\lambda R(x,y)} dxdy \text{, or} \quad (1)$$

$$\mathbf{E}(u,v,r) = -\frac{1}{2\pi} \iint_{T_x \times T_y} \frac{\partial \mathbf{E}}{\partial z}(x,y,0) \frac{e^{-jkR(x,y)}}{R(x,y)} dxdy \text{,} \quad (2)$$

where **E** is complex electric field amplitude; λ is wavelength, k=2π/λ; u=sinα, v=cosα sinβ, w=cosα cosβ are direction cosines of the direction of observation, β and α are azimuth and elevation of the direction of observation, r is the distance between the origin and observation point; U, V, W and R are directional cosines and length of the vector between integration point and observation point.

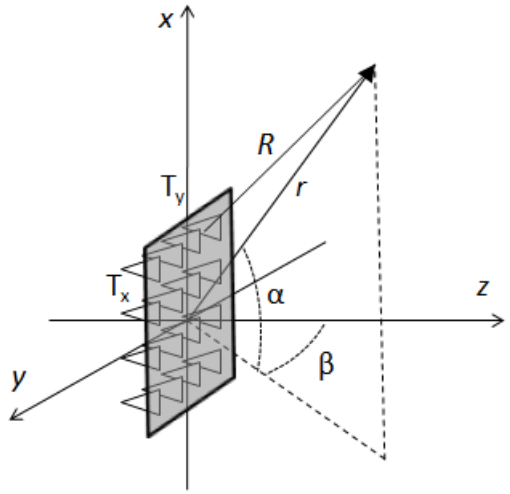

Figure 1: Antenna and the reference frame.

Under the condition $kR \gg 1$, the error of (1) and (2) is determined by the same integrals over the region $\mathbb{R}^2 \setminus T_xxT_y$. If the rectangle T_xxT_y includes all points with significant (large enough) amplitude of the field, then the error is small.

The further analysis will be based on (2). Analysis can be carried out based on (1) as well. As it will be shown, the result will change insignificantly in this case.

Let us make a simplification for the case, when the observation point is at least as far as in the Fresnel region, i.e.:

$$r > 0.62\sqrt{D^3/\lambda} \text{.} \quad (3)$$

In this case (2) can be rewritten in the following way:

$$\mathbf{E}(u,v,r) = -\frac{e^{-jkr}}{2\pi r} \iint_{T_x \times T_y} \frac{\partial \mathbf{E}}{\partial z}(x,y,0) \times e^{-j\Phi_r(x,y,u,v)} dxdy \text{,} \quad (4)$$

where

$$\Phi_r(x,y,u,v) = k\sqrt{(ru-x)^2 + (rv-y)^2 + r^2(1-u^2-v^2)} - kr \approx -k(xu+yv) + \frac{k}{2r}\left(x^2(1-u^2) + y^2\left(1-v^2\right) - 2xyuv\right)$$

$$= \Phi^{(1)}(x,y,u,v) + \Phi_r^{(2)}(x,y,u,v) \text{,} \quad (5)$$

$$\Phi^{(1)}(x,y,u,v) = -k(xu+yv) \text{,} \quad (6)$$

$$\Phi_r^{(2)}(x,y,u,v) = \frac{k}{2r}\left(x^2(1-u^2) + y^2\left(1-v^2\right) - 2xyuv\right). \quad (7)$$

3. Field transformation

We consider the following problem: given field measurements at a sphere r_1 in the Fresnel region, we need to determine field values at a sphere r_2. The problem of reconstructing far field corresponds to $r_2 \to \infty$.

3.1. Transformation theory

Consider the following representation of exponential of the phase function from (4) for the sphere r_2:

$$e^{-j\Phi_{r2}(x,y,u,v)} = g(x,y,u,v)e^{-j\Phi_{r1}(x,y,u,v)} \text{,} \quad (8)$$

where

$$g(x,y,u,v) = \exp\left(j\frac{k}{2}\left(\frac{1}{r_1} - \frac{1}{r_2}\right) \times \left(x^2(1-u^2) + y^2\left(1-v^2\right) - 2xyuv\right)\right) \quad (9)$$

Let us expand (9) into Fourier series as a function of (x,y) at a rectangle $[-T_x/2,T_x/2]$x$[-T_y/2,T_y/2]$ for fixed u and v:

$$g(x,y,u,v) = \sum_{m,n} k_{mn}(u,v) e^{jm\frac{2\pi}{T_x}x} e^{jn\frac{2\pi}{T_y}y} \text{,} \quad (10)$$

where

$$k_{mn}(u,v) = \frac{1}{T_xT_y} \iint_{T_x \times T_y} e^{j\frac{k}{2}\left(\frac{1}{r_1} - \frac{1}{r_2}\right)\left(x^2(1-u^2) + y^2\left(1-v^2\right) - 2xyuv\right)} \times e^{-jm\frac{2\pi}{T_x}x} e^{-jn\frac{2\pi}{T_y}y} dxdy \text{.} \quad (11)$$

Substitute (10) into (8) taking into account denotations (6) and (7):

$$e^{-j\Phi_{r2}(x,y,u,v)} = \sum_{m,n} k_{mn}(u,v) e^{jm\frac{2\pi}{T_x}x} e^{jn\frac{2\pi}{T_y}y} e^{-j\Phi_{r1}(x,y,u,v)} \approx \sum_{m,n} k_{mn}(u,v) e^{-j\Phi^{(1)}(x,y,u+m\Delta u,v+n\Delta v)} e^{-j\Phi_{r1}^{(2)}(x,y,u,v)} \text{.} \quad (12)$$

where

$$\Delta u = \lambda / T_x \text{,}\ \Delta v = \lambda / T_y \text{.} \quad (13)$$

For r_1 in the Fresnel region, in the vicinity of u, v the following inequality takes place:

$$\left|\Phi^{(2)}_{r_1}(x,y,u,v) - \Phi^{(2)}_{r_1}\left(x,y,u+m\Delta u, v+n\Delta v\right)\right| \ll 1. \quad (14)$$

With (14), the relation (12) can be rewritten as:

$$e^{-j\Phi_{r2}(x,y,u,v)} \approx \sum_{m,n} k_{mn}(u,v) e^{-j\Phi_{r1}(x,y,u+m\Delta u, v+n\Delta v)}. \quad (15)$$

Note, that physical interpretation of (15) is representation of a spherical wave with center in (u,v,r_2) as a linear combination of spherical waves with centers in $(u+m\Delta u, v+n\Delta v, r_1)$, the representation taking place at a rectangle T_xxT_y.

Now substitute (15) into (4). After changing order of summation and integration, we have:

$$\mathbf{E}(u,v,r_2) \approx e^{-jk(r_2-r_1)} \frac{r_1}{r_2} \times \sum_{m,n} k_{mn}(u,v) \mathbf{E}(u+m\Delta u, v+n\Delta v, r_1). \quad (16)$$

In sum (16) only several terms contribute significantly, so other terms can be dropped. This issue will be considered in more detail below.

Note, that a formula analogous to (16) was originally obtained in [13] for a two-dimensional problem and later in [14] for a three-dimensional problem for the case when antenna is illuminated by a nonplanar wave. However in these publications the formulas were applied only to nonplanar waves of a compact range.

Now let us consider a point u_2, v_2, which is located between nodes $u_1+m\Delta u$, $v_1+n\Delta v$. Let the node u_1, v_1 be the closest node of the mentioned grid's nodes to u_2, v_2. Expression (8) can be rewritten as:

$$e^{-j\Phi_{r2}(x,y,u_2,v_2)} = g(x,y,u_1,v_1,u_2,v_2) e^{-j\Phi_{r1}(x,y,u_1,v_1)}. \quad (17)$$

After transformations similar to (10)-(16), we obtain:

$$\mathbf{E}(u_2,v_2,r_2) \approx e^{-jk(r_2-r_1)} \frac{r_1}{r_2} \sum_{m,n} k_{mn}(u_1,v_1,u_2,v_2) \times \mathbf{E}(u_1+m\Delta u, v_1+n\Delta v, r_1), \quad (18)$$

where

$$k_{mn}(u_1,v_1,u_2,v_2) = \frac{1}{T_x T_y} \iint_{T_x \times T_y} e^{j\Phi^{(2)}_{r1}(x,y,u_1,v_1) - j\Phi^{(2)}_{r2}(x,y,u_2,v_2)} \times e^{jk(x(u_2-u_1)+y(v_2-v_1))} e^{-jm\frac{2\pi}{T_x}x} e^{-jn\frac{2\pi}{T_y}y} dxdy. \quad (19)$$

Note, that in (18) the largest contribution into sum is made by the field samples near (u_2,v_2), because coefficients (19) have largest magnitudes in this area.

Thereby, using field values in the angular grid $u_1+m\Delta u$, $v_1+n\Delta v$ on a sphere in Fresnel region or far region, one can reconstruct field values in every points of the half-space in Fresnel region or far region. Formulas (18),(19) can also be generalized for the case when r_1 and/or r_2 are in antenna near zone. This issue will be considered in the following publications. Also, (18),(19) can be applied at closer distances than indicated by (3). In [12] it was shown that these formulas can be applied under the following conditions:

$$\frac{D^4}{50\lambda r^3} << 1, \ \frac{D}{4r} << 1. \quad (20)$$

Note, that if we base the formulas on (1) instead of (2), then (18) turns into:

$$\mathbf{E}(u_2,v_2,r_2) \approx e^{-jk(r_2-r_1)} \frac{r_1}{r_2} \sum_{m,n} \frac{w_2}{w_{1,mn}} k_{mn}(u_1,v_1,u_2,v_2) \times \mathbf{E}(u_1+m\Delta u, v_1+n\Delta v, r_1), \quad (21)$$

where

$$w_{1,mn} = \sqrt{1-(u_1+m\Delta u)^2-(v_1+n\Delta v)^2}. \quad (22)$$

The formula for coefficients in this case remains the same – (19). Formula (21) is also very close to (18), since $w_2/w_{1,mn}$ are close to 1. Numerical simulation also shows that the formulas work equally well.

The formulas can also be applied to samples equally spaced in azimuth-elevation coordinates. Let us show it for the case when either $\alpha \approx 0$ or $\beta \approx 0$. In this case the phase doesn't have an *xy* term, so the two-dimensional integral (19) becomes a product of two one-dimensional integrals and the formula takes simpler form.

First, consider $\alpha \approx 0$ (when field is measured in azimuth sections). Then field values are given in a rectangular grid in α-β:

$$\alpha = \alpha_1 + m\Delta u, \beta = \beta_1 + n\Delta v, \ \alpha_1 \approx 0. \quad (23)$$

These angles correspond to the following *u* and *v*:

$$u \approx \alpha_1 + m\Delta u, v = \sin(\beta_1 + n\Delta v), \quad (24)$$

i.e. *v* spacing becomes smaller when azimuth increases. Based on (13), to have a smaller spacing for *v* we need to increase the area for integration: $\tilde{T}_y = T_y / \cos(\beta)$. Substituting it into (19) yields:

$$k_{mn} = \frac{1}{T_x T_y} \int_{-T_x/2}^{T_x/2} e^{j\frac{k}{2}\left(\frac{1}{r_1}-\frac{1}{r_2}\right)x^2 + jkx(\alpha_2-\alpha_1)} e^{-jm\frac{2\pi}{T_x}x} dx \times \int_{-T_y/2}^{T_y/2} e^{j\frac{k}{2}\left(\frac{1}{r_1}-\frac{1}{r_2}\right)y^2 + jky(\beta_2-\beta_1)} e^{-jn\frac{2\pi}{T_y}y} dy. \quad (25)$$

Using same considerations one can obtain the formula for $\beta \approx 0$ (elevation section):

$$k_{mn} = \frac{1}{T_x T_y} \int_{-T_x/2}^{T_x/2} e^{j\frac{k}{2}\left(\frac{1}{r_1}-\frac{1}{r_2}\right)x^2 + jkx(\alpha_2-\alpha_1)} e^{-jm\frac{2\pi}{T_x}x} dx \times \int_{-T_y/2}^{T_y/2} e^{j\frac{k}{2}\left(\frac{1}{r_1}-\frac{1}{r_2}\right)y^2/\cos^2\alpha_1 + jky(\beta_2-\beta_1)/\cos\alpha_1} e^{-jn\frac{2\pi}{T_y}y} dy. \quad (26)$$

Also note, that all formulas were written in vector form so far. However, one doesn't need to measure all three components of the field. Firstly, it is not necessary to measure radial component since in Fresnel region it is small and in addition its influence on far field is reduced due to the fact that in (18) radial components are almost orthogonal to transversal components of the far field.

Also, (18) can be used in scalar form separately for co and cross components of the field. It is also due to the fact that in (18) only points with close angular directions are used, so basis vectors of co and cross polarizations are almost orthogonal, regardless of which pair of co and cross polarizations is used.

3.2. Analogies

Let us draw several analogies with other results of antenna measurements theory. First, let us apply (18),(19) for $r_1 = r_2$. In this case the formulas become interpolation formulas with sampling functions; the coefficients tend to:

$$k_{mn}(u_1,v_1,u_2,v_2)\big|_{r_1=r_2} \approx \operatorname{sinc}\left(\frac{\pi}{\Delta u}(u_2-(u_1+m\Delta u))\right) \times \operatorname{sinc}\left(\frac{\pi}{\Delta v}(v_2-(v_1+n\Delta v))\right). \quad (27)$$

This result was achieved in [15], [16]. Note, that there is a small difference between formulas, which is due to different mathematical models of the field. We consider models (1) and (2) more appropriate, because in the model used in [15] equivalent magnetic currents on the virtual aperture were not taken into account. However, numerical simulation shows that both models work equally well.

Note, that field interpolation formulas can be used in the far field reconstruction problem the following way. The field can be reconstructed with (18),(19) in sparse angular grid with spacing Δu, Δv from (13). Then interpolation formulas can be applied to determine field values between nodes of the grid.

Also the formulas similar to those obtained in the previous section can be found based on field integration on a spherical surface. To obtain such representation one can apply interpolation formulas to the field on a sphere, at which the measurements take place. Let us show this approach in scalar approximation. The field on a sphere $r_2>r_1$ in direction u_2, v_2 can be represented using field on a sphere r_1 in the Fresnel region:

$$E(u_2,v_2,r_2) = j\iint E(u,v,r_1)\frac{r_1^2 e^{-jk\Delta r(u,v)}}{\lambda\Delta r}d\Omega, \quad (28)$$

where $\Delta r(u,v)= |\mathbf{r}_2(u_2,v_2)-\mathbf{r}_1(u,v)|$.

Using formulas for field interpolation in Fresnel region it can be rewritten as (with $u_1= v_1=0$ for simplicity):

$$E(u_2,v_2,r_2) = j\iint \sum_{m,n} E(m\Delta u,n\Delta v,r_1) \times \frac{\sin((u-m\Delta u)\pi/\Delta u)}{(u-m\Delta u)\pi/\Delta u}\frac{\sin((v-m\Delta v)\pi/\Delta v)}{(v-m\Delta v)\pi/\Delta v} \times \frac{r_1^2 e^{-jk\Delta r(u,v)}}{\lambda\Delta r(u,v)}d\Omega \quad (29)$$

After changing the order of summation and integration and regrouping, the formula can be written as:

$$E(u_2,v_2,r_2) = e^{-jk(r_2-r_1)}\frac{r_1}{r_2} \times \sum_{m,n}\tilde{k}_{mn}E(m\Delta u,n\Delta v,r_1), \quad (30)$$

where

$$\tilde{k}_{mn} = j\iint \frac{\sin((u-m\Delta u)\pi/\Delta u)}{(u-m\Delta u)\pi/\Delta u} \times \frac{\sin((v-m\Delta v)\pi/\Delta v)}{(v-m\Delta v)\pi/\Delta v}\frac{r_1 r_2 e^{jk(r_2-r_1)-jk\Delta r(u,v)}}{\lambda\Delta r(u,v)}d\Omega. \quad (31)$$

Despite the difference between formulas (31) and (19), numerical evaluation shows that the coefficients coincide with high precision. Note, that a similar approach was used in near field to far field transformation in [17], where measurements on cylindrical surface were considered.

Finally, let us show that formulas obtained in [4], are a special case of (18) and (19) when $u_1=u_2\approx 0$, $v_1=v_2\approx 0$, $r_2\to\infty$. In the notations of this paper, the formulas from [4] can be written as:

$$\mathbf{I}(s\Delta u,t\Delta v,r_2) \approx \sum_{m,n}\hat{k}_{mn}\mathbf{I}((s+m)\Delta u,(t+n)\Delta v,r_1), \quad (32)$$

where $\mathbf{I}$ is a vector potential, and $\hat{k}_{mn}$ are:

$$\hat{k}_{mn} = \frac{1}{T_x T_y}\int_{-T_x/2}^{T_x/2} e^{j\frac{k}{2r_1}x^2} e^{-jm\frac{2\pi}{T_x}x}dx \times \int_{-T_y/2}^{T_y/2} e^{j\frac{k}{2r_1}y^2} e^{-jn\frac{2\pi}{T_y}y}dy. \quad (33)$$

With small u and v the vector potential $\mathbf{I}$ defined in [4] is proportional to the electric field vector $\mathbf{E}$. One can see that formulas (25) and (26) tend to (33) when $u_1=u_2\approx 0$, $v_1=v_2\approx 0$, $r_2\to\infty$. Note, that (25) uses azimuth and elevation angular variables as opposed to (33), which uses u and v; it makes (25) more precise for directions distant from the normal to the aperture.

3.3. The amount of sections

The k_{mn} coefficients rapidly decrease with m and n, as can be seen from Fig.2. Also, field in Fresnel region decreases as the observation point moves away from field maximum. Therefore, in sums (16), (18) a finite number of terms can be used. Let us estimate minimum amount of terms for correct far field reconstruction.

At first, consider a well-focused antenna with maximum along Z-axis, when central azimuth section is reconstructed. For field reconstruction M azimuth sections of the field in the Fresnel region are measured. To estimate $M_{\min}$ let us use a stationary phase method. The integrals defining k_{mn} and $E(m\Delta u,n\Delta v,r_1)$ have a stationary phase point under conditions $|m|\le T_x^2/(2\lambda r_1)$ and $|n|\le T_y^2/(2\lambda r_1)$. Hence, estimation for the amount of sections is [9]:

$$M_{\min} = 2\left[\frac{T_x^2}{2\lambda r_1}\right]+1. \quad (34)$$

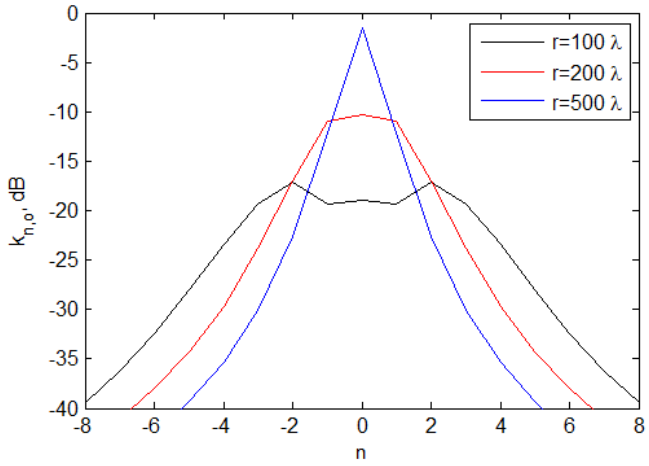

Figure 2. Magnitudes of $k_{n,0}$ coefficients for antenna with size 30 λ and different r.

However, the amount of n-terms shouldn't be limited with this estimation. It is due to contribution of the points with largest field amplitudes in Fresnel region to sums (16), (18) even for points distant from field maximum in far zone. Such terms have small k_{mn} but large $E(u+m\Delta u,v+n\Delta v,r_1)$, so they should also be included into the summation.

A similar effect takes place when a reconstructed section doesn't go through field maximum: in this case in addition to (34) it might be required to measure the sections which go through Fresnel field maximum. Also (34) cannot be applied to badly focused antennas (e.g. antennas with contoured beams), because estimation of the size of Fresnel field maximum made above might be incorrect in this case.

Note, that formula (34) is an estimation, which means that to obtain a more precise result it might be required to measure several additional sections.

3.4. Gain, EIRP and *G*/*T* calculation

Using the presented field transformation formulas it is possible determine antenna gain [10]. Since Poynting vector can be expressed as $\Pi=|E|^2/(60\pi)$, antenna gain can be determined by:

$$G(u,v)=\frac{4\pi r_2^2\Pi}{P}=\frac{|E(u,v,r_2)|^2\ r_2^2}{60P}, \qquad (35)$$

where P is antenna input power, $r_2>2D^2/\lambda$.

Substituting (18) to (35), gives:

$$G(u,v)=\frac{\left|r_1\sum_{m,n}k_{mn}E(u+m\Delta u,v+n\Delta v,r_1)\right|^2}{60P}. \qquad (36)$$

In (35), (36) the symbol E designates field amplitude at the given polarization, expressed in V/m. Since in practice the field is measured in non-calibrated units, one can use an auxiliary standard antenna with a known gain for calibration.

It is more convenient to use a standard antenna with far field distance smaller than r_1. In this case the AUT gain is:

$$G(u,v)=\frac{P_0G_0}{P}\times\left|\frac{1}{E_0}\sum_{m,n}k_{mn}E(u+m\Delta u,v+n\Delta v,r_1)\right|^2, \qquad (37)$$

where P_0, G_0, E_0 are input power, gain and measured non-calibrated field amplitude of the standard antenna.

If the AUT is an active antenna, one can determine its EIRP:

$$PG(u,v)=P_0G_0\times\left|\frac{1}{E_0}\sum_{m,n}k_{mn}E(u+m\Delta u,v+n\Delta v,r_1)\right|^2. \qquad (38)$$

Formulas (37),(38) are for a transmitting AUT. A similar formula for antenna gain can be written for a receiving AUT (according to reciprocity principle, measurements in transmitting mode and in receiving mode are equivalent). If an auxiliary transmitting antenna is working with a constant power, AUT gain is:

$$G(u,v)=G_0\times\left|\frac{1}{E_0}\sum_{m,n}k_{mn}E(u+m\Delta u,v+n\Delta v,r_1)\right|^2. \qquad (39)$$

The AUT noise quality G/T can be determined using [18]:

$$\frac{G(u,v)}{T}=\frac{4\pi k\Delta f}{\lambda^2}\frac{4\pi r_1^2}{P_tG_t}\times\frac{1}{2N}\left|\sum_{m,n}k_{mn}E(u+m\Delta u,v+n\Delta v,r_1)\right|^2, \qquad (40)$$

where k is Boltzmann constant, Δf is effective bandwidth, P_t and G_t are power and gain of the transmitting antenna, N is noise power at AUT.

4. Computer simulation results

In this section the results of computer simulation are presented. For simulation an axisymmetrical reflector antenna was used, D=30λ ($2D^2/\lambda$=1800λ). Using PO approximation several azimuth sections of Fresnel field at 200λ and a central section of far field were calculated. Elevation spacing was 1.8°. Based on (18), (19) far field was reconstructed and compared to the calculated far field. Fig.3 shows the results of field reconstruction using 7 sections of Fresnel field (according to (34)) and 11 sections, and a central section of the Fresnel field. For the first case the gain error was 0.03 dB, first side lobe level error was 0.4 dB. For the second case the gain error was 0.01 dB, first side lobe level error was 0.07 dB.

5. Configuration of the measurement system

To carry out measurements the AUT is adjusted to a positioner, which must be able to rotate in both azimuth and elevation (Fig.4). Measurement system configuration for AUT in receiving mode is shown in Fig.5.

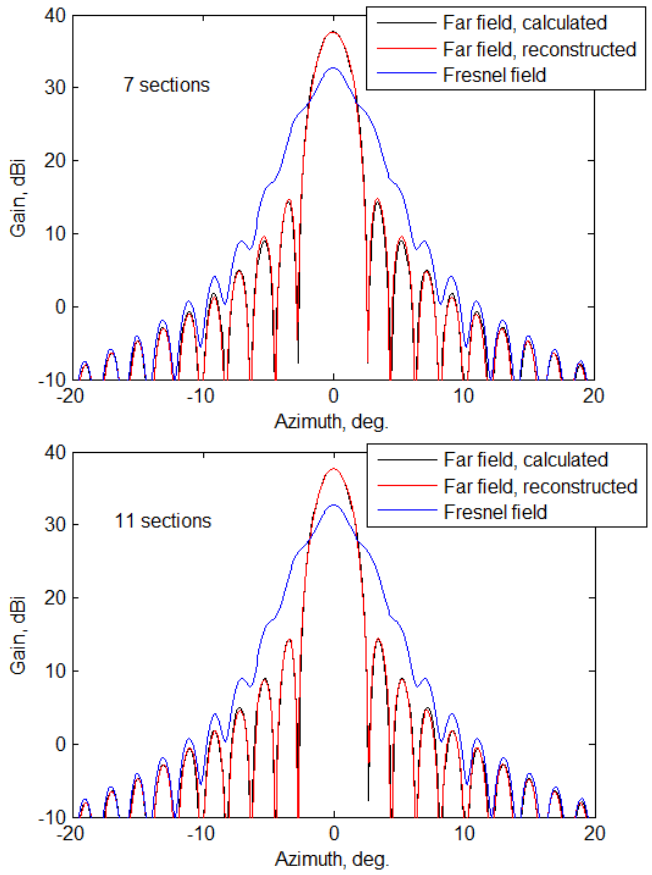

Figure 3: Computer simulation results using 7 sections and 11 sections in Fresnel region.

The AUT 5 receives the signal transmitted by an auxiliary antenna 2. For phase measurements a reference channel with an auxiliary receiving antenna 3 is used. Amplitude and phase of the received signal are registered in circuit analyzer 10 and stored in computer 12 for current positioning angles. The measurements take place when the positioner gradually changes its azimuth with a fixed elevation. After the section is measured, positioner changes elevation and then the measurements continue. After that the data are processed using (18) and (19) or (25)/(26).

For gain measurements the input of the mixer 7 is switched to a standard antenna 6 and then field amplitude in the maximum of standard antenna's radiation pattern is measured. Antenna gain is determined using (39). To measure gain or EIRP of a transmitting antenna the configuration shown in Fig.5 is modified accordingly.

6. Experimental verification

For verification of the method a set of experiments was carried out [9]. Field patterns of an offset reflector antenna with D=0.6 m at f=12.5 GHz ($2D^2/\lambda$=30m) with linear polarization were measured in an anechoic chamber. The measurements were taken at different distances: in far region at 76 m and in Fresnel region. In Fresnel region several elevation sections of the field with azimuth spacing 2^o were taken. Then reconstructed far field was compared to measured far field.

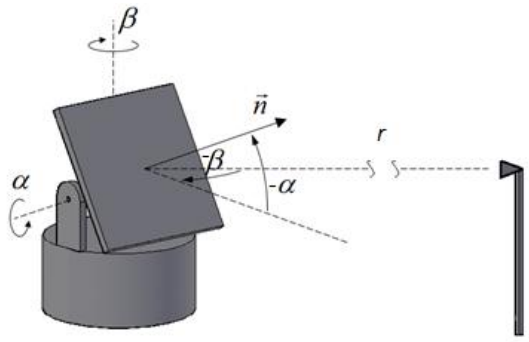

Figure 4: Antenna on a positioner.

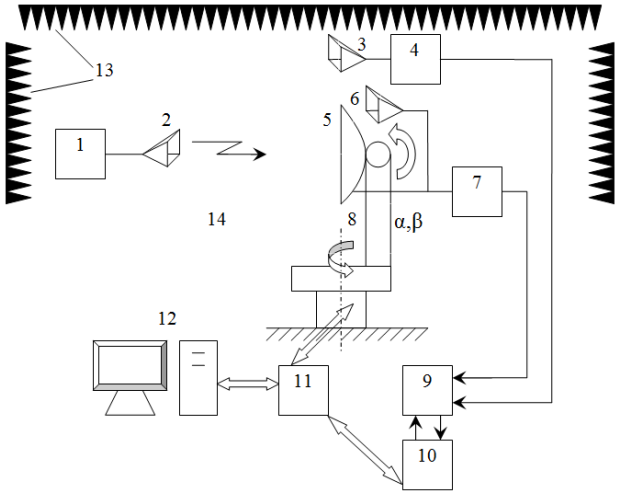

Figure 5: Configuration of the measurement system (simplified): 1 – generator; 2 – auxiliary transmitting antenna; 3 – reference channel antenna; 4 – reference channel mixer; 5 – AUT; 6 – standard antenna; 7 – measurements channel mixer; 8 – positioner; 9 – amplification an commutation unit; 10 – vector circuit analyzer; 11 – controller; 12 – computer; 13 – RAM; 14 – anechoic chamber.

In Fig.6 the results of far field reconstruction using 7 sections measured at 4 m and using 9 sections at 2.5 m are given. Comparing the reconstructed and measured radiation patterns one can see that the quality of reconstruction is good and the error is less than 3 dB in the dynamic range up to -50 dB. Error of maximum side lobe level reconstruction is 1 dB and 0.3 dB for 4 m and 2.5 m measurements.

Fig.7 shows the results of cross-polarization reconstruction using measurements at 7.6 m. The reconstructed pattern also agrees with the measured one.

The method described in this article has been used for antenna measurements in an anechoic chamber in company Radiofizika (measurements distance up to 80 m) for several years. Using this method many antennas were tested, with far field distance of hundreds of meters and even kilometers. Fig.8 shows the increase of maximum size of antennas, which can be tested in the anechoic chamber of Radiofizika, that is gained when Fresnel field measurements instead of far field measurements are used. The lower curve corresponds to the standard far field criterion $r>2D^2/\lambda$, the higher curve corresponds to criterion (20).

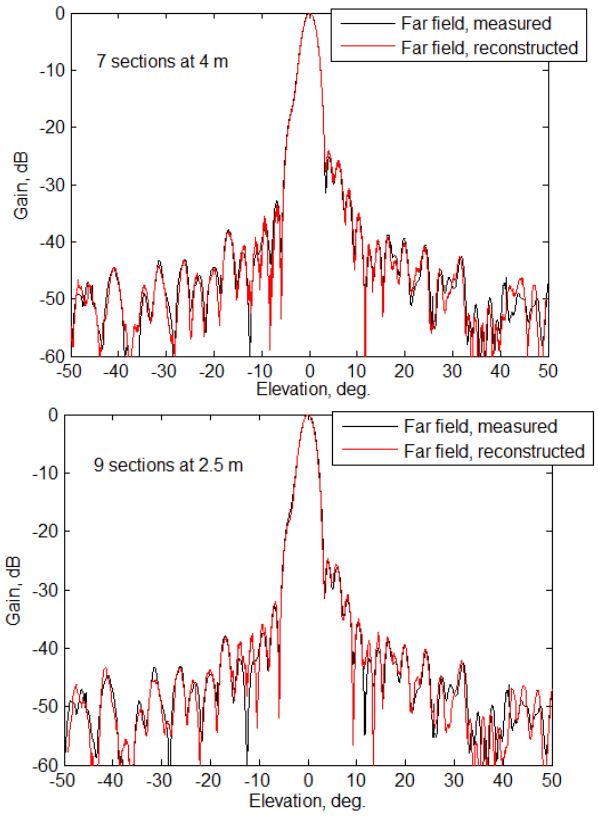

Figure 6. Experimental verification results (co-polarization).

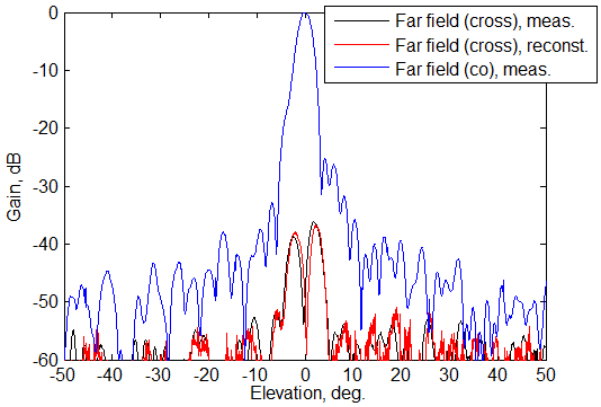

Figure 7. Experimental verification results (cross-polarization).

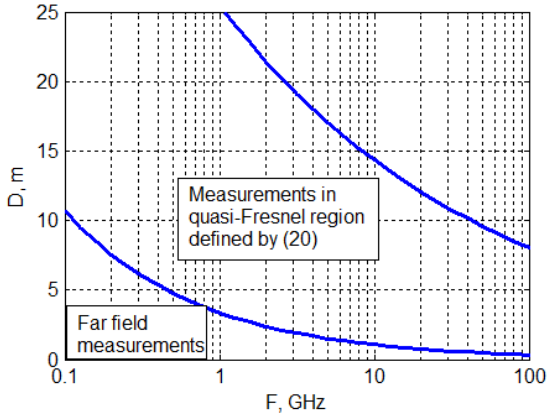

Figure 8. Maximum size of antennas, which can be tested in the anechoic chamber of Radiofizika, versus frequency.

Fig.9 demonstrates the example of far field reconstruction for a reflector antenna (D=3.8m). The antenna adjusted on a positioner is shown in Fig.10. Far field distance of the antenna at f=6.25 GHz is 600m. Measurement distance was 76 m, i.e. 8 times less.

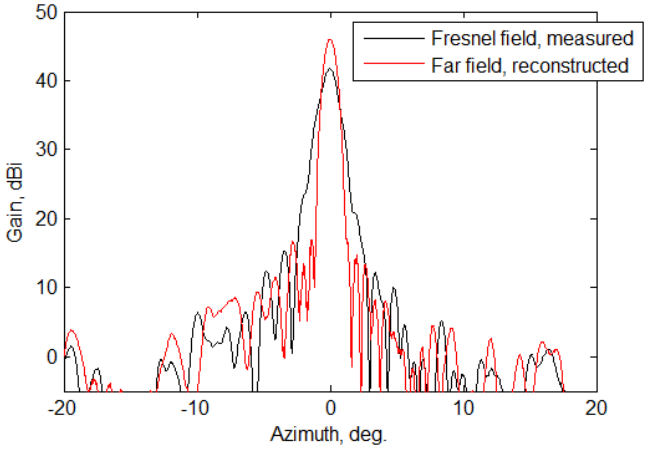

Figure 9. Reconstructed far field and central section of the measured Fresnel field for antenna D=3.8m, f=6.25GHz.

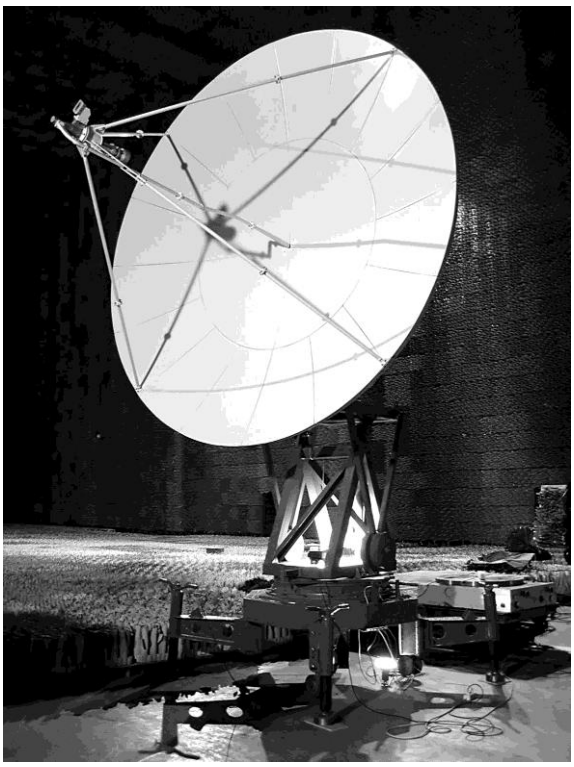

Figure 10. C-band reflector antenna (D=3.8m) on a positioner.

7. Conclusions

Fresnel field to far field transformation based on two-dimensional Fourier series expansion was presented. The method was compared to other results from antenna measurements theory. The results of computer simulation and experimental verification were presented. The results

suggest that the method ensures good quality of far field reconstruction. The method has been used in practice in an anechoic chamber of company Radiofizika for over 12 years for measurements of large-size antennas, and it has obvious advantages over outdoor far field measurements.

References

[1] R. Mittra, W. Imbriale, Gain and pattern measurements of large aperture antennas in the Fresnel zone, *Proc. IEEE APS Digest*, 1969, vol. 7, pp. 40-42.

[2] Yu.A. Kolosov, A.P. Kurochkin, Radiation pattern reconstruction using field known in a limited angular sector, *Antennas*, vol.16, 1972, pp. 25-37 (in Russian).

[3] G. D'Elia, G. Leone, R. Pierri, A new approach in the near field-far field transformation. *Proc. IEEE APS Digest*, Houston, USA, 1983, pp. 495-498.

[4] G. D'Elia, G. Leone, R. Pierri, G. Schirinzi, New Method of Far-Field Reconstruction from Fresnel Field, *Electronics Letters*, vol. 20, no. 8, Apr. 1984, pp. 342-343.

[5] G. Evans, Far Field Correction for Short Antenna Ranges, *Proc. AMTA Symposium*, 1985, pp. 34.1–34.9.

[6] G. Evans, *Antenna Measurement Techniques*, Artech House, 1990.

[7] M. Sierra-Castañer, S. Burgos, Fresnel zone to far field algorithm for rapid array antenna measurements, *Proc. EuCAP Symposium*, Rome, Italy, April 2011, pp. 3251-3255.

[8] K. Wu, S. Parekh, A method of transforming Fresnel field to far field for circular aperture antennas, *Proc. IEEE APS Digest*, May 1990, pp. 216–219.

[9] I.L. Vilenko, A.A. Meduhin, Yu.A. Suserov, A.K. Tobolev, A.V. Shishlov, Reconstruction of antenna radiation pattern by using data of measurements in a Fresnel region with test facility intended for far-field measurements, *Antennas*, vol. 1(92), pp. 46–52, 2005 (in Russian).

[10] S.-S. Oh, J.-M. Kim, J.-H. Yun, Antenna measurement on cylindrical surface in Fresnel region using direct far-field measurement system, *ETRI J.*, vol. 29, no. 2, pp. 135–142, 2007.

[11] S.-S. Oh, J.-H. Yun, New Method for Predicting the Electromagnetic Field at a Finite Distance Using Fresnel Field Transformation, *IEEE Antennas and Wireless Propagation Letters*, vol. 7, pp. 291–293, 2008.

[12] Yu.V. Krivosheev, A.V. Shishlov, Development of the method of antenna radiation pattern reconstruction using measurements in the Fresnel zone, *Proc. Radars and Communication*, Moscow, Russia, November 2010, pp. 320-324 (in Russian).

[13] L. D. Bakhrakh, I. V. Kaplun, A. P. Kurochkin, Determination of Parameters of Antennas Illuminated by a Nonplanar Wave, *Radio Engineering and Electronic Physics*, vol. 20, Dec. 1975, pp. 1-8. Translation from Russian.

[14] L.D. Bakhrakh, S.D. Kremenetskiy, A.P. Kurochkin, V.A. Usin, Ya.S. Shifrin, *Near field antenna measurements*, Nauka, 1985 (in Russian).

[15] O. Bucci, G. Franceschetti, G. D'Elia, Fast analysis of large antennas – A new computational philosophy, *IEEE Transactions on Antennas and Propagation*, vol. 28 , 1980, pp. 306 – 310.

[16] G. D'Elia, G. Leone, R. Pierri, D. Valentino, Numerical evaluation of the near field using sampling expansions, *Proc. IEEE APS Digest*, 1982, vol.20, pp. 241 – 244.

[17] O. Bucci, C. Gennarelli, Use of sampling expansions in near-field-far-field transformation: the cylindrical case. *IEEE Transactions on Antennas and Propagation*, vol. 36, 1988, pp. 830 – 835.

[18] E.N. Egorov, *Basics of microwave electronics*, 1983 (in Russian).